

A FINITE STATE AUTOMATON MODEL FOR MULTI-NEURON SIMULATIONS

Maria Schilstra[†], Alistair Rust^{‡§}, Rod Adams[‡] and Hamid Bolouri^{†¶}

[†] Science and Technology Research Centre, University of Hertfordshire, UK

[‡] Department of Computer Science, University of Hertfordshire, UK

[§] European Bioinformatics Institute, Cambridge, UK

[¶] Division of Biology, California Institute of Technology, USA

Keywords: Finite state automaton, dendrite morphology, computer simulation, excitation propagation

Abstract

‘Classical’ compartmental modelling techniques involve numerical solution of large sets of ordinary differential equations (ODEs). The computational cost of neuronal network evaluation using these techniques forms a major bottleneck in the exploration of the effects of dendrite morphology on network functionality. To reduce computational load, we have developed a finite state automaton model of membrane activity, which will potentially permit the evaluation and comparison of large numbers of simulated 3-dimensional networks. The automaton mimics the behaviour of 2-equation ODE models for wave propagation in excitable media, and was found to be capable of modelling the most important characteristics of neural membranes.

Motivation

The morphology of biological neurons plays a key role in their dynamic and adaptive computational capabilities [7]. We aim to explore the relationship between form and function, particularly in simulated networks of spatially extended neurons. It is hoped that this will lead to a better understanding of the principles that govern the development and dynamics of biological neural networks.

Previously, we have developed a biologically inspired methodology to simulate 3-dimensional neurite growth and the creation of inter-neuron connections within a virtual 3D space [11,13]. Local ‘chemical’ gradients, emitted by neurons or other sources, affect neural outgrowth according to a small number of developmental rules. Specific network architectures are evolved by optimising the parameters that control the developmental process, using an evolutionary computation method. A fully functional large-scale artificial neural network that simulated the functionality of an edge-detecting retina was evolved using this approach. Further, the methodology was employed to generate 3D dendritic structures that have spiking patterns similar to those of bursting stellate and pyramidal neurons [10]. Although the shapes of the evolved neurons were ostensibly quite different from those of the example neurons, their spiking behaviour was remarkably similar [12]. We therefore ask whether there are classes of neurite geometry with distinct electrophysiological characteristics.

To examine this issue, we need to generate and analyse large sets of neurons and neuronal networks, and investigate whether classification is possible. Our methodology for neurite development can be used to create single neurons as well as networks with functional characteristics akin to biological examples. However, the computational cost of evaluation using compartmental modelling techniques [1,6] that are based on solving large sets of ordinary differential equations (ODEs) forms a major bottleneck in the statistical exploration of the effects of morphology on functionality. We are, therefore, developing a simplified neural membrane model that is behaviourally equivalent to the current ODE-based models, and that, we hope, will permit faster evaluation of evolved 3-dimensional neurons and neuronal networks. Finite state automata are used routinely to model excitation wave propagation through so-called excitable media [2], and provide a fast, albeit often crude, alternative to numerical solution of differential equations. In this paper we describe the adaptation of an existing FSA to model action potential and dendritic spike propagation in tree-like structures.

The model

Two-equation ODE systems such as the FitzHugh-Nagumo or Morris-Lecar equations (see [8] for more information) are reduced forms of more general multi-dimensional equations that model voltage-gated ion

channels, such as the Hodgkin-Huxley equation. Gerhardt et al. [3,4] have shown that the behaviour of such reduced systems, which retain the main characteristics of the more complete systems, can be mimicked using a relatively simple FSA.

Both the Gerhardt FSA and the reduced ODE systems use two time dependent parameters, u and v , to describe the state of a compartment. The ‘excitation’ parameter u represents relatively fast physiological processes, such as Na^+ channel activation. Slower processes, such as K^+ channel activation, are combined in the ‘recovery’ parameter v . A compartment that has not been perturbed for some time is said to be ‘resting’. Upon a small perturbation of u , a compartment will quickly return to the resting state. However, when the perturbation exceeds a certain threshold, θ , the compartment will go through a typical cycle of excitation and recovery. At the beginning of the cycle, the perturbation becomes larger, but its proliferation is slowed down, halted, and reversed as a result of a recovery reaction (increase in v) that starts as a response to the increased perturbation. The recovery reaction itself also goes through a maximum and then decreases back to its resting level, but occurs on a slower timescale than the excitation. Furthermore, θ increases with v , so that recovering compartments have a reduced sensitivity to incoming stimuli. Thus, for some time after excitation of a compartment, its re-excitation is more difficult or even impossible. Perturbations may be caused by external sources, such as synapses, but, significantly, neighbouring compartments whose value of u is high can also provide an excitatory stimulus through ‘diffusion’. As a result, arrays of excitable compartments mimic the behaviour of excitable media, in which excitation waves can propagate undamped over long distances.

The FSA described here models wave propagation along finite tree-like structures with tapering branches, rather than along infinite or toroidal regular 2- or 3-dimensional arrays. It is, therefore, in several respects different from the FSAs that are routinely used to simulate wave propagation in excitable media [2]. The structure of our FSA model, and the rules that are used for updating are explained in more detail in Figures 1 and 2. As we will show below, our FSA models the main characteristics of neurites containing voltage-gated ion channels (for recent reviews of these characteristics see [5,8,14]).

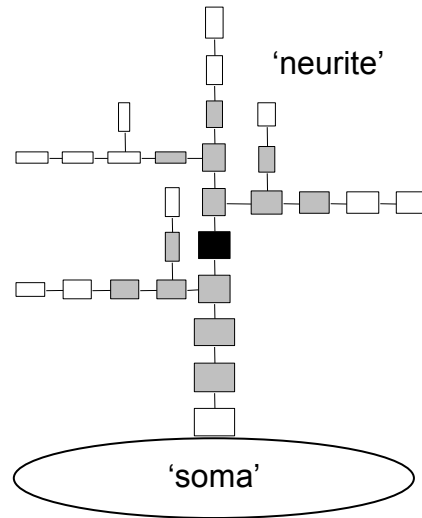


Figure 1. ‘Neurites’ are modelled as tree-shaped structures with cylindrical compartments that are connected at their roots to a ‘soma’. Compartments have unit length, but may have different diameters. All compartments in the structure are updated in synchrony, in a sequence of discrete time steps. The next state of a compartment is determined by e , the accumulated excitation of its neighbourhood. Here, the grey compartments and the black compartment itself form the neighbourhood of the black compartment, for a ‘neighbourhood radius’ $r = 3$. To account for the inhomogeneities in the structure (compartments may have different numbers of neighbours, and different diameters), the contributions of individual compartments to the accumulated neighbourhood excitation, e , are weighted according to their volume, surface area, or a combination of the two as follows: $e = \Sigma(D_i^P \cdot u_i) / \Sigma(D_i^P)$. Here, u_i is the value of u in the i^{th} compartment of the neighbourhood, and D_i^P the diameter D of that compartment, raised to the power P ($P = 0$: equal compartmental weights; $P = 1$: weights proportional to surface area; $P = 2$: weights proportional to volume; $P = 3/2$: combination of surface area and volume). Summations are done over all compartments in the neighbourhood. P and u_{max} , the maximum excitation level, are constant for all compartments in the structure.

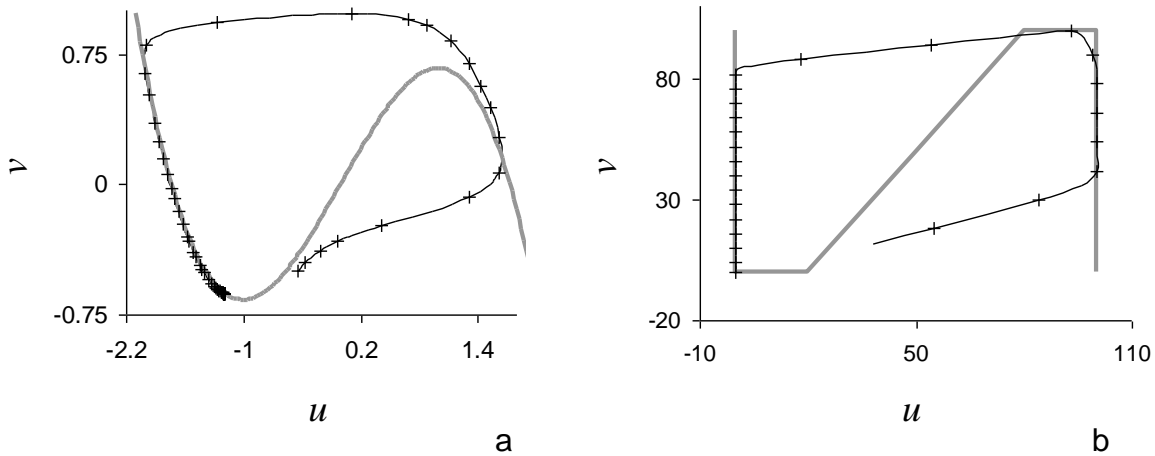


Figure 2. The compartments are updated according to the following rules. When the accumulated neighbourhood excitation e is above a certain threshold θ , the compartment is in the ‘excited’ state, and its u and v increase, until they reach their maximum values u_{max} and v_{max} ($u_{next} = \min\{u + g_u^{up}(v), u_{max}\}$, $v_{next} = \min\{v + g_v^{up}, v_{max}\}$). The value of θ increases with v ($\theta = \theta_0 + (\theta_1 - \theta_0)v/v_{max}$, in which θ_0 and θ_1 are the threshold values at $v = 0$ and $v = v_{max}$), and eventually becomes so high that the excited state cannot be maintained, and the compartment goes into ‘recovery’. In this state, the values of u and v decrease until they reach zero ($u_{next} = \max\{u - g_u^{down}(v), 0\}$, $v_{next} = \max\{v - g_v^{down}, 0\}$). The rate at which u rises and falls (g_u) is dependent on the current value of v ($g_u^{up} = g_u^{up_0}(1 - v/a)$, $g_u^{down} = g_u^{down_0} + (g_u^{down_1} - g_u^{down_0}) \times v/v_{max}$, where $g_u^{up_0}$ and $g_u^{down_0}$ are the values of g_u^{up} and g_u^{down} at $v = 0$, and $g_u^{down_{max}}$ is g_u^{down} at $v = v_{max}$, and a is a constant). Parameter values used in the simulations presented here were $u_{max} = v_{max} = 100$, $\theta_0 = 20$, $\theta_1 = 80$, $g_u^{up_0} = 20$, $g_u^{down_0} = 3$, $g_u^{down_1} = 20$, $g_v^{up} = 6$, $g_v^{down} = 3$, $a = 80$, $r = 1$, $P = 2$). Changes in v tend to lag behind changes in u , because v rises and falls more slowly than u . Here, the phase-plane portrait of the FitzHugh-Nagumo model (a, equations and parameter values as in [7]) is compared with that of the FSA model (b). The thick grey lines indicate the u -nullclines (at which $g_u(v)$ changes sign). The black lines in both diagrams indicate typical trajectories of u and v after excitation of the compartment. Both trajectories start at the points inside circles, and follow the trajectories indicated by the arrows. Crosses indicate units of time.

Model behaviour

General characteristics

Neurites simulated with the FSA approach described above have the following characteristics:

- Injecting a brief excitatory pulse of u into a single compartment results in two waves (‘action potentials’, or ‘dendritic spikes’) of elevated u and v , moving in opposite directions away from the point of injection. In a linear stretch of neurite with a uniform diameter the propagation rate is determined by the rates at which u and v are allowed to change, and by the value of θ .
- Continuous excitation results in wave trains. This is because v , and therefore θ , decrease only slowly, and a compartment is effectively unexcitable for some time after it has made the transition from excited to recovering.
- A wave that reaches a tip fades away without being reflected. Two equally sized waves that travel in opposite directions toward each other along a single branch of uniform diameter annihilate each other.

This behaviour is characteristic for all excitable media. It is independent of the detailed arrangement of the compartments, and occurs in one- and higher dimensional, regular and irregular assemblies. This behaviour is also characteristic for axons and neurites, provided the density of voltage-gated channels along their length is sufficiently high, and local voltage thresholds are sufficiently low to permit spike initiation.

Characteristics specific for tree-shaped structures

Neurites, and in particular dendrites, are highly diverse, both in structure and in function. Some of the heterogeneity is due to differences in the distribution of voltage-gated channels along the length of the

structures. However, dendrites with different morphologies, but built from identical compartments, can show very different behaviour [10]. This diversity must ultimately be due to differences in the cable structure of the dendrites, and to the fact that signals can constructively or destructively interfere. In passive cable structures, dendritic branch points attenuate spikes that propagate toward the soma, and the result is that spikes propagate more readily away from the soma than in the opposite direction [1,8,14]. This behaviour underlies all other (including that of active neurites), and any model should reproduce it.

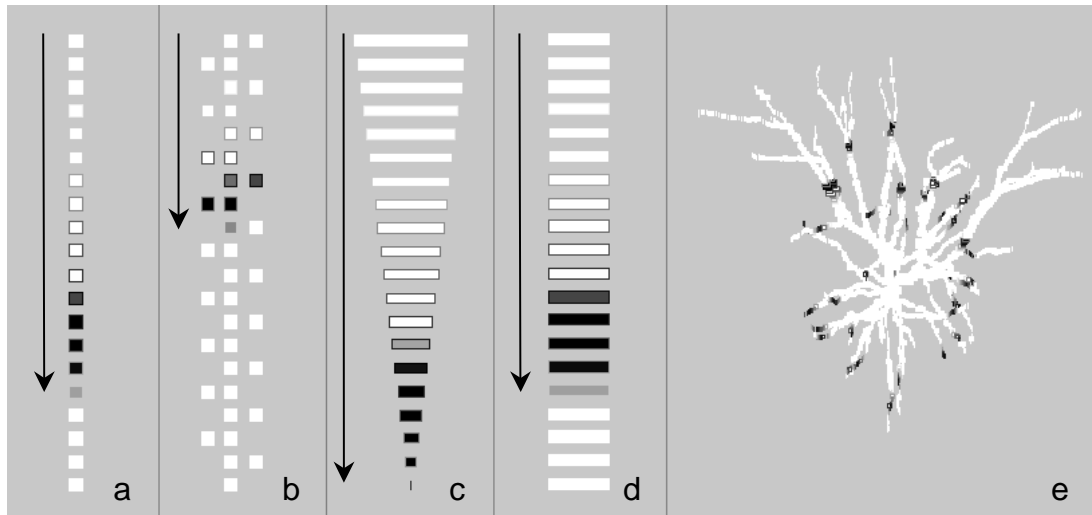


Figure 3. Relative wave velocity is determined by the branching pattern and the degree of tapering of the branches. Structures *a*, *b*, *c*, and *d* are ‘neurites’ that have received a brief (1 propagation round) excitatory pulse into their top compartments. All structures were updated 50 times, and the resulting excitation wave moved from the top downwards. The length of all compartments is 1.0, their diameters 1.0 (*a*, *b*), 5.0 (*d*) or vary from 10.0 at the top to 0.5 at the bottom compartment (*c*). The darker the fill of a compartment, the higher the excitation parameter u , the darker its outline, the higher the recovery parameter v . Notice that increases in v lag behind increases in u . In the uniform structures *a* and *d*, the front of excitation wave is at compartment 16, showing that the width of the neurite has no effect on wave velocity. However, in the highly branched structure *b*, wave velocity is significantly lower (the wave front is at compartment 9), whereas the wave has moved faster through the tapering structure (wave front at compartment 20). Panel *e* shows a excitation wave, backpropagating from the soma, along the dendrites of a layer 2/3 neocortical pyramidal neuron (compartmentalisation as in [10]), modelled with our FSA. The snapshot was taken 300 updates after a brief excitatory pulse was applied to the dendrite compartments directly adjacent to the soma.

In the FSA described here, the cable structure is taken into account as follows. The ‘next’ state of a resting compartment is determined by the accumulated excitation of all cells in its neighbourhood (fig. 1). We assume that the maximum excitation is the same in all compartments, so that the amplitude of the waves is always the same. However, not all compartments in a neighbourhood have the same size, and the number of neighbours may be different from compartment to compartment. It is reasonable to assume that u spreads from compartment to compartment through lateral interactions (‘diffusion’), and that ‘dilution’ of the transferred excitation increases at branching points (provided the sum of the diameters of the daughter compartments is greater than the diameter of the parent). The dilution factor may be proportional to the ratio of the compartmental volumes before and after the branching point, to the ratio of the surface areas, or to a combination of the two. The FSA model incorporates the effect of differences in structure by weighting the contributions of individual compartments to the accumulated neighbourhood excitation (see fig. 1). The consequences are the following:

- When a wave reaches a branching point where the surface area or volume increases, it will experience a momentary delay, and may even terminate (Figure 3a and b). This happens because the effective excitation threshold increases at the branching point. The result is that waves travel more slowly through a highly branched structure than through a linear one. Furthermore, wave trains, generated by continuous excitation of a single compartment, have equal temporal frequencies, but their spatial frequencies increase with the degree of branching. In general,

branched structures are open for waves spreading towards distal regions, allowing spike back propagation from the soma, but tend to be blocking for waves travelling towards the soma. This kind of behaviour is required in models of the dendritic tree as logical network (e.g. [9]).

- Waves move with uniform velocity through linear structures with compartments that have equal diameters, and this velocity is independent of the actual diameter value. However, in tapering linear structures, in which the compartmental diameters decrease, a wave's velocity increases when it moves towards the narrower compartments, and decreases when it moves in the opposite direction. Therefore, a pulse that spreads outwards from the soma speeds up when it moves towards the distal branches. (Figure 3c and d).
- Passive membrane can be modelled by setting the excitation threshold to a value that can never be reached. In that case, any excitation transferred into a compartment will simply dilute further, and eventually leak away.
- Two waves that travel up different daughter branches and coincide at the branching point can reinforce each other and travel further towards the root as a single wave ('coincidence detection', see [5] and references therein). Waves may also travel up a branch, and meet and annihilate a wave going in the opposite direction. In general, simultaneous excitation of several non-consecutive compartments in a branched structure will result in interference patterns at some other point in the structure. Non-simultaneous excitation may also result in wave interference, as long as the effects of the excitations overlap. An example of an interference pattern generated by continuous 'synaptic' excitation at points distributed over the branches of a relatively simple neurite is shown in Figure 4. Interference patterns generated in this way are strongly dependent on the individual positions of the synapses.

The behaviour described above is characteristic for tree structures, and does not occur in regular arrays.

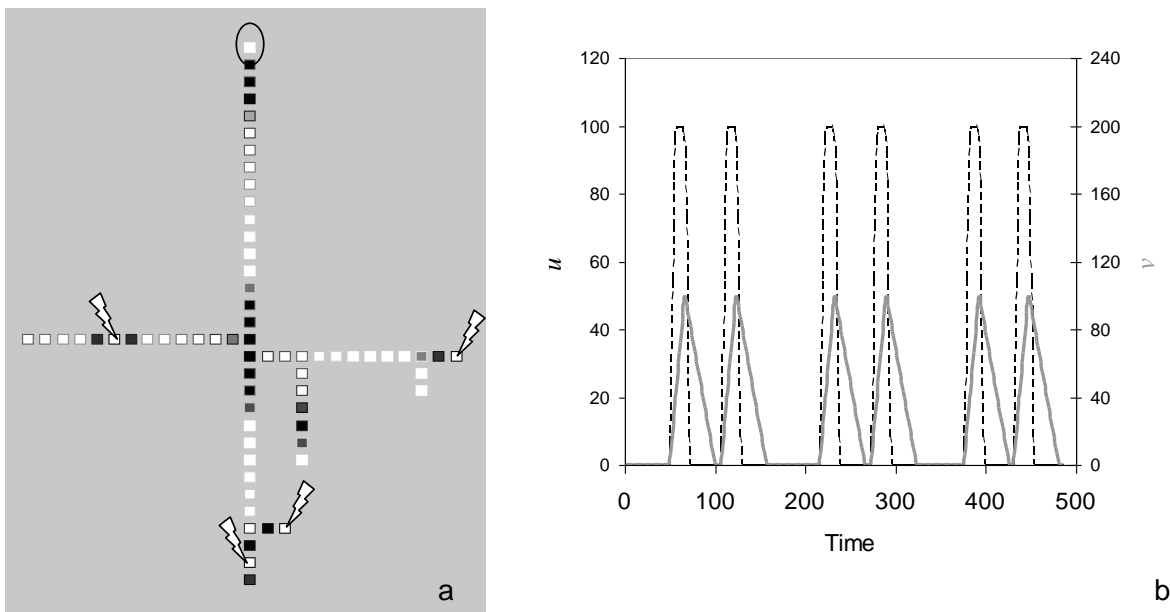


Figure 4. Interference of excitation waves. Compartments connected to the four 'synapses', indicated by lightning symbols in the structure shown on the left, were continuously excited. The resulting interference pattern, monitored at the compartment indicated by the ellipse, is shown on the right. Dashed black and solid grey lines indicates u (values on left Y-axis) and v (values on secondary Y-axis), respectively.

Conclusion

The results presented in this paper demonstrate that the FSA approach described here models the basic properties of active and passive neurites. Because each compartment can assume only a limited number of states, the time required for evaluation of whole neurons such as the one in Figure 3 is significantly shorter than the evaluation time required by classical approaches. From the times required to generate

spike patterns, we estimate that the FSA approach is at least ten times faster than ODE-based techniques. A significant further improvement may be expected from parallel implementation of the FSA. We are currently making a detailed comparison of the FSA model with the traditional compartmental models, in order to make sure that none of the observed phenomena are actually artefacts of the simplifications that we have made. We also would like to pinpoint the strengths and limitations of our approach. For instance, at present our FSA cannot be used to simulate intrinsically bursting neurons, because there is no mechanism to generate an afterdepolarising potential ([8,10]). If the outcome of our tests is satisfactory, we plan to integrate the FSA model with our method for generating 3-dimensional neural networks. We hope that this approach will provide an effective tool for exploring the basic relationships between neural form and network function in statistically large numbers of simulated 3-dimensional networks.

References

- [1] J.M. Bower and D. Beeman, *The book of GENESIS* (Springer, Berlin, Germany, 1997).
- [2] B. Ermentrout and L. Edelstein-Keshet, Cellular automata approaches to biological modelling, *J. Theor. Biol.* 160 (1993) 97-133.
- [3] M. Gerhardt, H. Schuster and J.J. Tyson, A cellular automaton model of excitable media including curvature and dispersion, *Science* 247 (1990) 1563-1566.
- [4] M. Gerhardt, H. Schuster and J.J. Tyson, A cellular automaton model of excitable media. II. Curvature, dispersion, rotating and meandering waves, *Physica D* 46 (1990) 392-415.
- [5] M. Häusser, N. Spuston and G.J. Stuart, Diversity and dynamics of dendritic signalling, *Science* 290 (2000) 739-744.
- [6] M. Hines and N. Carnevale, The NEURON simulation environment, *Neural Computation* 9 (1997) 1179-1209.
- [7] C. Koch, Computation and the single neuron, *Nature* 385 (1997) 207-210.
- [8] C. Koch, *Biophysics of computation* (Oxford University Press, New York, 2000).
- [9] C. Koch, T. Poggio and V. Torre, Retinal ganglion cells: a functional interpretation of dendritic morphology, *Phil. Trans. Roy. Soc. B* 298 (1982) 227-264.
- [10] Z.F. Mainen and T.J. Sejnowski, Influence of dendritic structure on firing pattern in model neocortical neurons, *Nature* 382 (1996) 363-366.
- [11] A. Rust, R. Adams, S. George and H. Bolouri, Towards computational neural systems through development evolution. in: Wermter, S., Austin, J., and Willshaw, D. eds., *Emergent neural computational architectures based on neuroscience*, (Springer, Heidelberg, 2001) 188-202.
- [12] A.G. Rust and R. Adams, Developmental evolution of dendritic morphology in a multi-compartmental neuron model in: 9th International Conference on Artificial Neural Networks (ICANN'99), Vol. 1, (IEE, 1999) 383-388.
- [13] A.G. Rust, R. Adams, S. George and H. Bolouri, Developmental Evolution of an Edge Detecting Retina in: Niklasson, L., Boden, M., and Ziemke, T. eds., 8th International Conference on Artificial Neural Networks (ICANN'98), Vol. 2, (Springer, 1998) 561-566.
- [14] I. Segev and M. London, Untangling dendrites with quantitative modelling, *Science* 290 (2001) 745-750.